















sample displacement  $q_k$  and velocity  $\dot{q}_k$ ;  $w_k$  is the process noise due to disturbances and modelling inaccuracies;  $v_k$  is the measurement noise due to sensor inaccuracy. Following assumption  $w_k$  and  $v_k$  is zero mean and with covariance matrix:

$$E \left[ \begin{pmatrix} w_p \\ v_p \end{pmatrix} \begin{pmatrix} w_q^T & v_q^T \end{pmatrix} \right] = \begin{pmatrix} Q & S \\ S^T & R \end{pmatrix} \delta_{pq} \quad (9)$$

where the index  $p$  and  $q$  are time-instants;  $E$  is the expected value;  $\delta_{pq}$  is the Kronecker delta. As the correlation  $E(w_p w_q^T)$  and  $E(v_p v_q^T)$  are equal zero in case of different time-instant. Further the stochastic model is assumed that  $\{x_k\}$ ,  $\{w_k\}$  and  $\{v_k\}$  are mutual independent:  $E(x_k w_k^T)=0$  and  $E(x_k v_k^T)=0$ . According to Peeters & Roeck (1999) proven that the output covariance  $R=E[y_{k+i} y_k^T]$  for any arbitrary time-lags  $i$   $t$  can be considered as impulse response (Eq. 10) of the deterministic linear time-invariance system  $A, C, G$ ; where  $G= E[x_{k+1} y_k^T]$  is the next state-output covariance matrix.

$$R_i = CA^{i-1}G \quad (10)$$

The classification of SSI based on the key step of these methods; by following Peeters & Roeck (1999), they are covariance-driven stochastic subspace identification (COV-SSI) and data-driven stochastic subspace identification (DATA-SSI). In this study the DATA-SSI used to extract FDs.

#### 4.2 DATA-SSI

DATA-SSI works directly with time-series of experimental data, without need to convert out-put data to correlation, covariance or spectra. The main step of DATA-SSI is a projection of the row space of the future outputs into the row of past outputs. The orthogonal projection  $P_i$  is defined as:

$$P_i = Y_f / Y_p = Y_f Y_p (Y_p Y_p^T)^{-1} Y_p \quad (11)$$

Where the matrix  $Y_f$  and  $Y_p$  are the under half part and upper part half of a block Hankel matrix  $H$ , defined as:

$$H = \begin{bmatrix} Y_{(1:j-2i)} \\ Y_{(2:j-2i+1)} \\ \dots \\ Y_{(2i:j)} \end{bmatrix} = \begin{bmatrix} Y_p \\ Y_f \end{bmatrix} \begin{matrix} \Downarrow li \\ \Downarrow li \end{matrix} \quad (12)$$

where  $2i$  are the number of block rows,  $j$  are the number of data points,  $l$  are the number of output sensors. The main theorem of stochastic subspace identification states that the projection  $P_i$  can be factorized as the product of observability matrix  $O_i$  and the Kalman filter state sequence  $\hat{X}_i$  (Peeters & Roeck 1999):

$$P_i = \begin{pmatrix} C \\ CA \\ \dots \\ CA^{i-1} \end{pmatrix} \begin{pmatrix} \hat{x} & \hat{x}_{i+1} & \dots & \hat{x}_{i+j-1} \end{pmatrix} = O_i \hat{X}_i \quad (13)$$

The observability matrix  $O_i$  and the Kalman filter sequence  $\hat{X}_i$  are obtained by applying SVD to the projection matrix:

$$P_i = U_1 S_1 V_1^T \quad (14)$$

Combining Eq. (13) and Eq. (14) gives:

$$O_i = U_1 S_1^{1/2}, \quad \hat{X}_i = O_i^+ P_i \quad (15)$$

If the shifted past and future outputs of Hankal matrix another project is obtained:

$$P_{i-1} = Y_f^- / Y_p^+ = O_{i-1} \hat{X}_{i+1} \quad (16)$$

$O_{i-1}$  is obtained from  $O_i$  after deleting the last  $l$  rows and the shifted state sequence can be computed in Eq. (16) as:

$$\hat{X}_{i+1} = O_{i-1}^+ P_{i-1} \quad (17)$$

From Eq. (15) and Eq. (17), the Kalman state sequences  $\hat{X}_i, \hat{X}_{i+1}$  are calculated using only output data. The system matrices can now be recovered from over determined set of linear equations, obtained by extending Eq. (8):

$$\begin{pmatrix} \hat{X}_{i+1} \\ Y_{i/i} \end{pmatrix} = \begin{pmatrix} A \\ C \end{pmatrix} \begin{pmatrix} \hat{X}_i \end{pmatrix} + \begin{pmatrix} \rho_w \\ \rho_v \end{pmatrix} \quad (18)$$

where  $Y_{i/i}$  is a Hankel matrix with only one block row. Since the Kalman state sequence and the outputs are known and the residual  $(\rho_w \quad \rho_v)^T$  are uncorrelated with  $\hat{X}_i$ , the set of equation can be solved for A,C in a least-squares:

$$\begin{pmatrix} A \\ C \end{pmatrix} = \begin{pmatrix} \hat{X}_{i+1} \\ Y_{i/i} \end{pmatrix} \begin{pmatrix} \hat{X}_i \end{pmatrix}^+ \quad (19)$$

#### 4.3 Identification of flutter derivatives

The modal parameters of system can be obtained by solving the eigenvalue problem state matrix A (Eq. 19):

$$A = \Psi \Lambda \Psi^{-1}; \quad \Phi = C \Psi \quad (20)$$

where  $\Psi$  the complex eigenvector;  $\Lambda$  the complex eigenvalue is the diagonal matrix;  $\Phi$

the mode shape matrix. When the complex modal parameters known, the gross damping  $C^e$  and gross stiffness  $K^e$  in Eq. (5) is determined by following:

$$[K^e \ C^e] = -M[\Phi\Lambda^2 \ \Phi^*(\Lambda^*)^2] \begin{bmatrix} \Phi & \Phi^* \\ \Phi\Lambda & \Phi^*\Lambda^* \end{bmatrix}^{-1} \quad (21)$$

Let

$$\bar{C}^e = M^{-1}C^e; \quad \bar{K}^e = M^{-1}K^e$$

$$\bar{C} = M^{-1}C^0; \quad \bar{K} = M^{-1}K^0$$

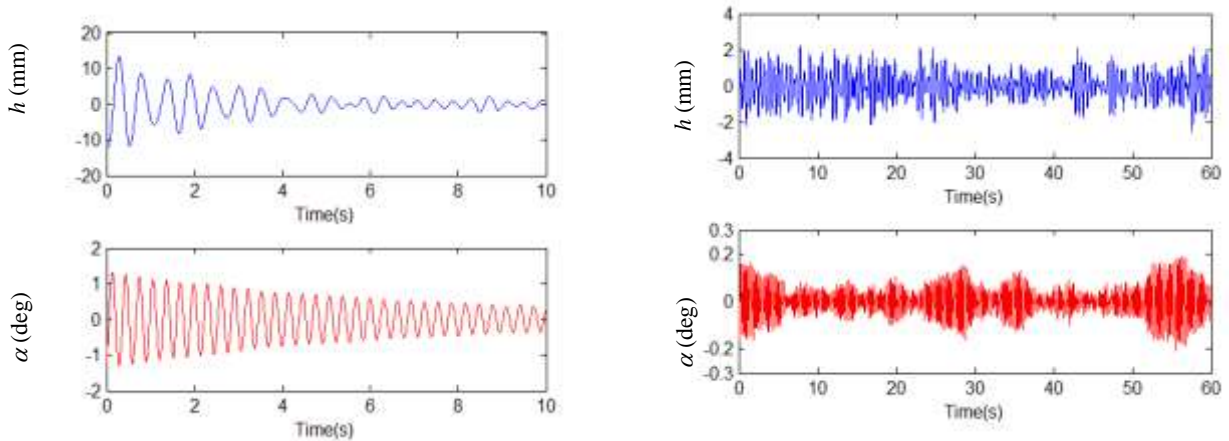
where  $C^0$  and  $K^0$  the mechanical damping and stiffness matrix of system under no-wind condition.

Thus, the flutter derivatives of two DOF can be defined as:

$$\begin{aligned} H_1^*(k_h) &= -\frac{2m}{\rho B^2 \omega_h} (\bar{C}_{11}^e - \bar{C}_{11}), & A_1^*(k_h) &= -\frac{2I}{\rho B^3 \omega_h} (\bar{C}_{21}^e - \bar{C}_{21}) \\ H_2^*(k_\alpha) &= -\frac{2m}{\rho B^3 \omega_\alpha} (\bar{C}_{12}^e - \bar{C}_{12}), & A_2^*(k_\alpha) &= -\frac{2I}{\rho B^4 \omega_\alpha} (\bar{C}_{22}^e - \bar{C}_{22}) \\ H_3^*(k_\alpha) &= -\frac{2m}{\rho B^3 \omega_\alpha^2} (\bar{K}_{12}^e - \bar{K}_{12}), & A_3^*(k_h) &= -\frac{2I}{\rho B^4 \omega_\alpha^2} (\bar{K}_{22}^e - \bar{K}_{22}) \\ H_4^*(k_h) &= -\frac{2m}{\rho B^3 \omega_h^2} (\bar{K}_{11}^e - \bar{K}_{11}), & A_4^*(k_h) &= -\frac{2I}{\rho B^4 \omega_h^2} (\bar{K}_{21}^e - \bar{K}_{21}) \end{aligned} \quad (22)$$

## 5. FLUTTER DERIVATIVES AND COMPARISON

The decay and buffeting responses are acquired at a sampling frequency 100Hz and these samples are zeros setting before to operating with Matlab (Fig. 6).



(a) Free decay response ( $V=5.3$ m/s)      (b) Buffeting response ( $V=5.3$ m/s)  
 Fig. 6 Response of the bridge deck section-model ( $h$ -vertical;  $\alpha$ -torsional)

### 5. 1 Extract of flutter derivatives from buffeting response

At high wind velocity, the aerodynamic damping of heaving mode is too high and vertical

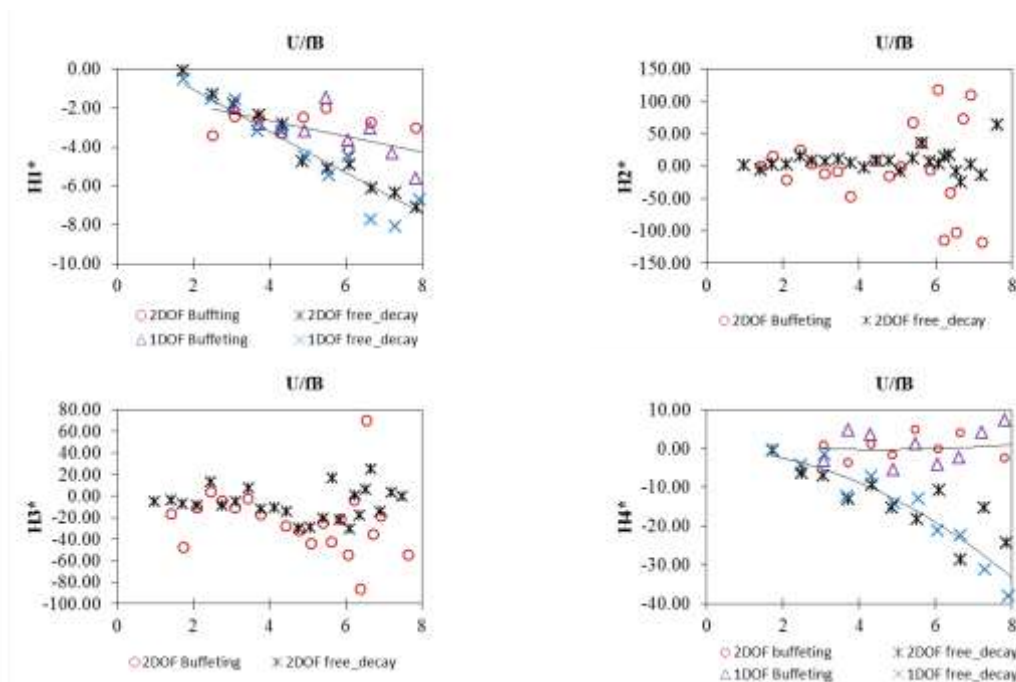


Fig. 7 FDs ( $H_i$ ) of the bridge section-model by SDOF test and coupled test by free decay and buffeting responses (case  $I_r=11.09\%$ )

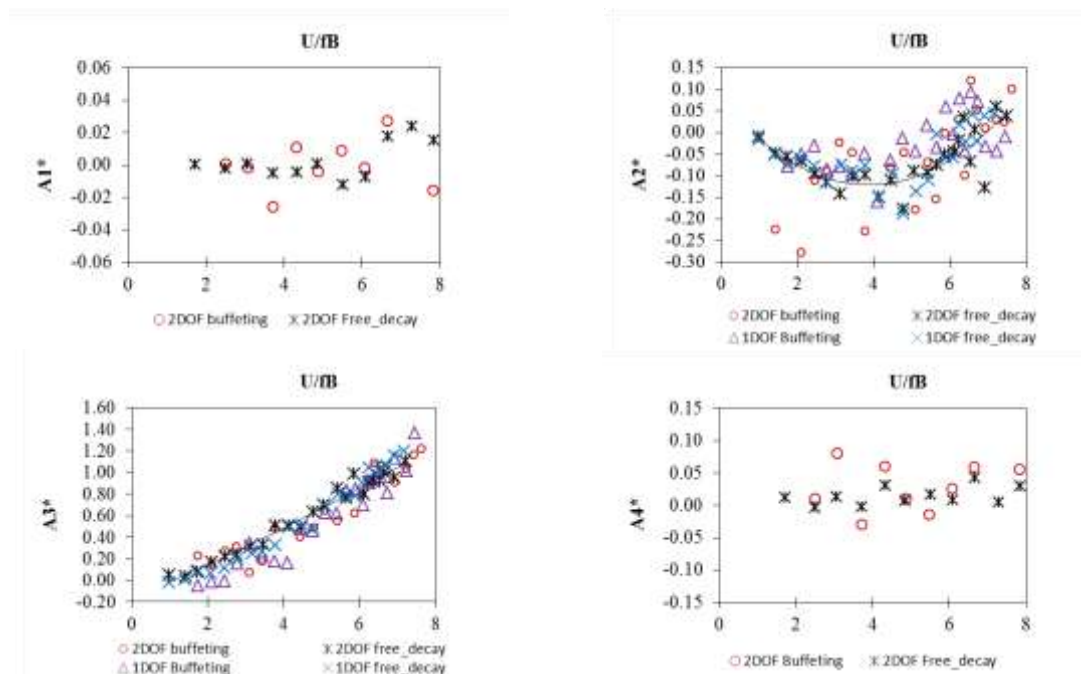
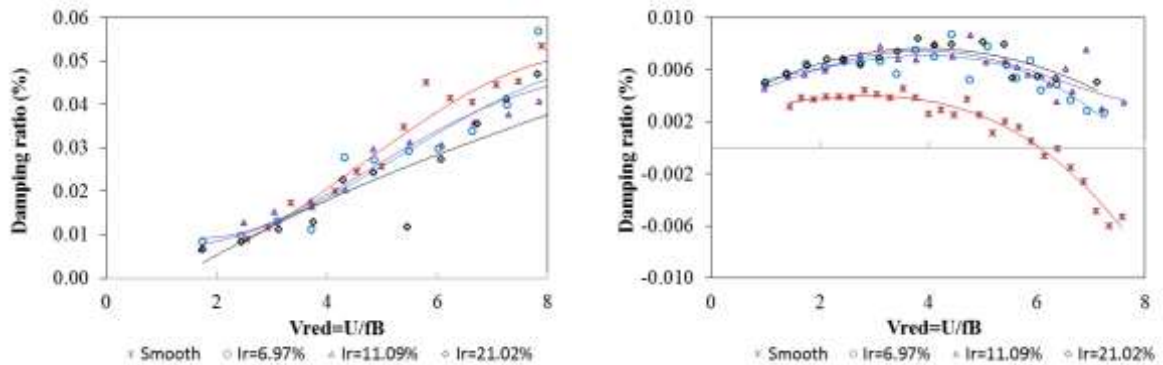


Fig. 8 FDs ( $A_i$ ) of the bridge section-model by SDOF test and coupled test by free decay and buffeting responses (case  $I_r=11.09\%$ )

free response is too short; therefore, the extraction of FDs cannot be accomplished high accuracy. The bridge deck section-model will vibrate under the excitation of turbulent flows even at small wind velocity, it is reasonable to extract FDs from buffeting response. Fig. 7&8 show the flutter derivatives of bridge deck by the DATA- SSI method from both free decay and buffeting responses of 1DOF and 2DOF systems under turbulence flows ( $I_r=11.09\%$ ). Overall, most FDs are in good agreement with both free decay and buffeting response of 1DOF and 2DOF systems, except FDs related to vertical frequency and vertical damping ( $H_1^*$  and  $H_4^*$ ). The difference may be explained by short data to recode under free decay test. The coupled aerodynamic derivatives ( $H_2^*$  and  $H_3^*$ ) extracted from buffeting responses are more scattering than from free decay, especially at high reduced wind speed. At small wind velocity, the amplitude of buffeting vibration is small and the high damping torsional mode is not fully excited, so the FDs is less accurate ( $A_2^*$ ).

### 5.2 The effects of turbulence on flutter derivatives

Fig. 10 & 11 illustrate the flutter derivatives of heaving and torsional mode under smooth and turbulent flows with the difference reduced turbulence intensity. In these derivatives, the torsional damping term  $A_2^*$ ; plays an important role on torsional flutter stability, since its positive/negative value corresponds to the aerodynamic instability/stability of torsional flutter. On the other hand, the coupled term,  $H_3^*$  and  $A_1^*$ , and the aerodynamically un-coupled derivative  $A_2^*$  have significant role on heaving-torsional of 2DOF coupled flutter instability (Matsumoto 2001). As shown in Fig. 9 & 11, under smooth flow, the positive value  $A_2^*$  at high reduced wind speed ( $V_{red}>5.5$ ) and total torsional damping are almost controlled by  $A_2^*$ , the coupling



a. Damping ratio of heaving mode                      b. Damping ratio of torsional mode  
 Fig. 9 Damping ratio of the bridge section-model under smooth and turbulence flows

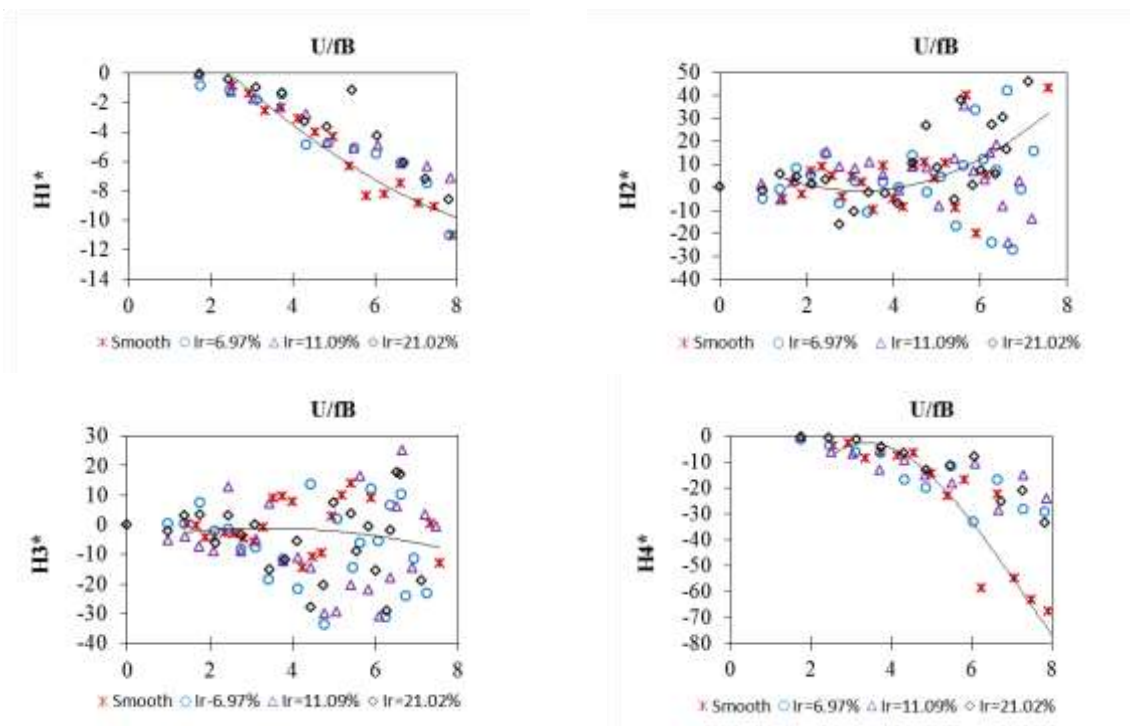
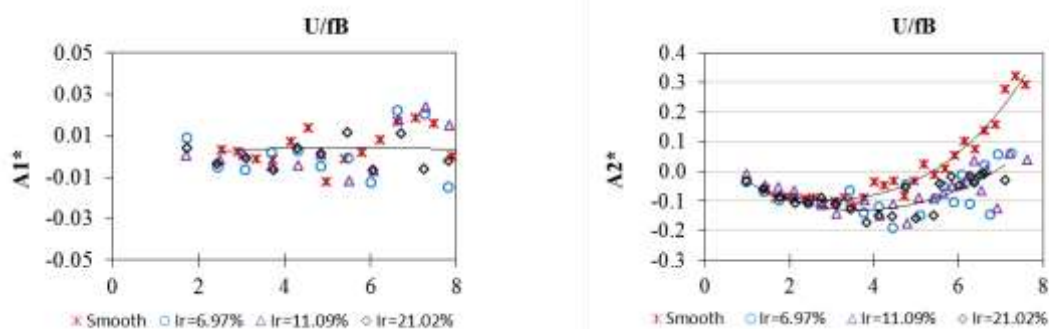


Fig. 10 FDs ( $H_i$ ) of the bridge section-model under smooth and turbulent flows by free decay response

such as  $H_3^*$  and  $A_1^*$  destabilize the torsional flutter. The significant effects of turbulence flows on flutter derivatives are also illustrated based on  $A_2^*$  term and aerodynamic torsional damping. However, the effects of different turbulence intensity on these aerodynamic terms are fairly modest. When there is an increase in the reduced turbulence intensity, the critical reduced velocity of torsional flutter is also increased (the possible value  $A_2^*$  corresponding turbulence:  $V_{red} = 6.8-7$  with  $I_r = 6.97\%$ ;  $V_{red} = 7.5$  with  $I_r = 11.09\%$ ; it is suitable compared with dynamic responses of bridge deck (Fig. 5). In general, flutter derivatives have a significant difference between smooth and turbulence flows, research of wind-induced vibration problems must be considered on this issue.



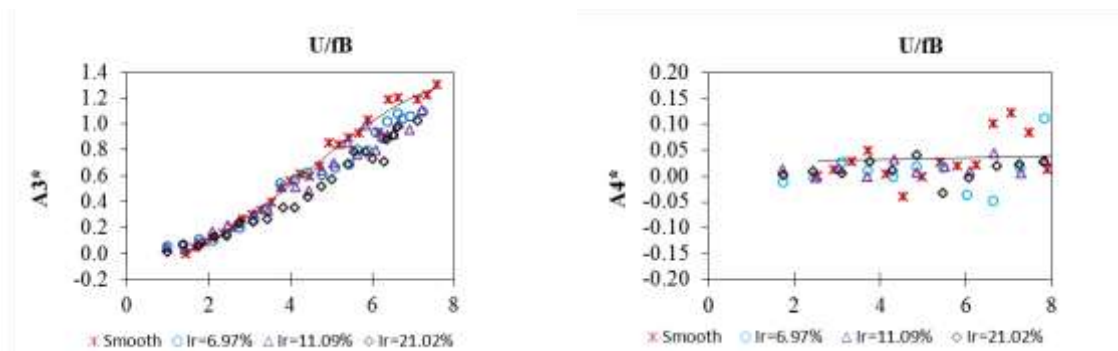


Fig. 11 FDs ( $A_i$ ) of the bridge section-model under smooth and turbulent flows by free decay response

## 6. CONCLUSIONS

This study investigated the effects of turbulence on flutter derivatives of trussed bridge deck section by using wind-tunnel test and out-put only state space stochastic system identification technique identified flutter derivatives from vary DOF and excitation. Conclusions from this study are summarized here:

DATA-SSI methods show a good result even under turbulence flows because an advantage of those methods is considered buffeting force and response as inputs instead of noises.

An identification of flutter derivatives from buffeting responses is plausible, the advantage of this technique is easier to obtain buffeting response, and the section-model will be oscillated under wind flow, moreover, in turbulence flows. This is less time consuming than free decay test. Especially at high wind velocity the vertical free decay data is too short, it is causes less accuracy.

Turbulence flows significantly affect on dynamic responses and flutter derivatives of trussed bridge deck section, specifically, turbulence induces larger displacement but increase critical divergence velocity are also illustrated based on buffeting response and aredynamic torsional damping term  $A_2^*$ .

Using the proposed framework, the variety of aerodynamic features were addressed, which helped us better understand the effect of different flows on aerodynamics of trussed bridge deck section.

## REFERENCES

- Bart Peeters and Guido De Roeck (1999), "Reference-based stochastic subspace identification for output-only modal analysis", *Mechanical Systems and Signal Processing*, 13(6), 855-878.
- Bartoli, G., Contri, S., Mannini, C. and Righi, M. (2009), "Toward an improvement in the identification of bridge deck flutter derivatives", *J. of Eng. Mech. ASCE*, Vol. 135, 771-785.
- Bartoli, G., Righi, M. (2006), "Flutter mechanism for rectangular prism in smooth and turbulent flow", *J. Wind Eng. Ind. Aerodyn*, Vol. 94, 275-291.

- Boonyapinyo, V., Janesupasaeree, T. (2010), "Data-driven stochastic subspace identification of flutter derivatives of bridge decks", *J. Wind Eng. Ind. Aerodyn*, Vol. 98, 784-799.
- Chowdhury, A.G., Sarkar, P.P. (2003), "A new technique for identification of eighteen flutter derivatives using three-degrees-of-freedom section model", *Engineering Structures*, Vol. 25, 1763-1772.
- Claes Dyrbye and Svend O. Hansen (1997), "Wind Loads on Structures", John Wiley & Sons, New York.
- Haan, F.L. (2000), "The effects of turbulence on the aerodynamics of long-span bridges", *Ph.D. Dissertation*; University of Notre Dame, US.
- Haan, F.L., Kareem, A. (2007), "The effects of turbulence on the aerodynamics of oscillating Prisms", *ICWE12 CAIRNS*, 1815-1822.
- Yamada, H., Miyata, T. and Ichikawa, H. (1992), "Measurement of aerodynamic coefficients by system identification method", *J. Wind Eng. Ind. Aerodyn*, Vol. 42, 1255-1263.
- Katsuchi, H. and Yamada, H. (2011), "Study on turbulence partial simulation for wind-tunnel testing of bridge deck", *Proc. of ICWE 13, Amsterdam, Netherlands*.
- Kirkegaard, P.H. and Andersen, P. (1997), "State space identification of civil engineering structures from output measurement", *Proc. of the 15th International Modal Analysis Conference*, Orlando, Florida, USA.
- Matsumoto, M., Tamwaki, Y. and Shijo, R. (2001), "Frequency characteristics in various flutter instabilities of bridge girders", *J. Wind Eng. Ind. Aerodyn*, Vol. 89, 385-408.
- Nikitas, N., Macdonal, J.H.G. and Jakobsen, J.B. (2011), "Identification of flutter derivatives from full-scale ambient vibration measurements of the Clifton suspension bridge", *J. Wind and Struct.*, Vol. 14, 221-238.
- Nakamura, Y. and Ozono, S. (1987), "The effects of turbulence on a separated and reattaching flow", *J. Fluid Mech.*, Vol. 178, 477-490.
- Scanlan, R.H. and Lin, W.H. (1978), "Effects of turbulence on bridge flutter derivatives", *J. Eng. Mech. Div.*, Vol.104, 719-733.
- Scanlan, R.H. (1997), "Amplitude and turbulence effects on bridge flutter derivatives", *J. Struct. Eng. ASCE*, Vol. 123, 232-236.
- Simiu, E. and Scanlan, R.H. (1996), "Wind Effects on Structures", 3rd edition, John Wiley & Sons, New York.
- Sarkar, P.P., Jones, N.P, Scanlan, R.H (1992), "System identification for estimation of flutter derivatives", *J. Wind Eng. Ind. Aerodyn*, Vol. 42, 1243-1254.
- Peeters B., and Roeck, G.D. (1999), Reference based stochastic subspace identification for output-only modal analysis", *Mech. Systems and Signal Processing*, (13(6)), 855-878.
- Juang, J.N., and Pappa, R.S. (1985), "An eigensystem realization algorithm (ERA) for modal parameter identification and model reduction", *J. Guid. Contr. Dyn.*, 299-318.
- Jakobsen, J.B, Hjorth-Hansen, E. (1995), "Determination of the aerodynamic derivatives by a system identification method", *J. Wind Eng. Ind. Aerodyn*, Vol. 57, 295-305.